



Plasticity of Carbohydrate Transport at the Blood-Brain Barrier

Ellen McMullen¹, Astrid Weiler¹, Holger M. Becker² and Stefanie Schirmeier^{1*}

¹ Department of Biology, Institute of Zoology, Technische Universität Dresden, Dresden, Germany, ² Division of General Zoology, Department of Biology, University of Kaiserslautern, Kaiserslautern, Germany

OPEN ACCESS

Edited by:

Jimena A. Sierralta,
University of Chile, Chile

Reviewed by:

Xavier Declèves,
Université Paris Descartes, France
Chul Hoon Kim,
Yonsei University, South Korea
Macarena Sánchez-Navarro,
Instituto de Parasitología y
Biomedicina López-Neyra
(IPBLN), Spain

*Correspondence:

Stefanie Schirmeier
stefanie.schirmeier@tu-dresden.de

Specialty section:

This article was submitted to
Pathological Conditions,
a section of the journal
Frontiers in Behavioral Neuroscience

Received: 30 September 2020

Accepted: 17 December 2020

Published: 22 January 2021

Citation:

McMullen E, Weiler A, Becker HM and
Schirmeier S (2021) Plasticity of
Carbohydrate Transport at the
Blood-Brain Barrier.
Front. Behav. Neurosci. 14:612430.
doi: 10.3389/fnbeh.2020.612430

Neuronal function is highly energy demanding, requiring efficient transport of nutrients into the central nervous system (CNS). Simultaneously the brain must be protected from the influx of unwanted solutes. Most of the energy is supplied from dietary sugars, delivered from circulation via the blood-brain barrier (BBB). Therefore, selective transporters are required to shuttle metabolites into the nervous system where they can be utilized. The *Drosophila* BBB is formed by perineurial and subperineurial glial cells, which effectively separate the brain from the surrounding hemolymph, maintaining a constant microenvironment. We identified two previously unknown BBB transporters, MFS3 (Major Facilitator Superfamily Transporter 3), located in the perineurial glial cells, and Pippin, found in both the perineurial and subperineurial glial cells. Both transporters facilitate uptake of circulating trehalose and glucose into the BBB-forming glial cells. RNA interference-mediated knockdown of these transporters leads to pupal lethality. However, null mutants reach adulthood, although they do show reduced lifespan and activity. Here, we report that both carbohydrate transport efficiency and resulting lethality found upon loss of MFS3 or Pippin are rescued via compensatory upregulation of Tret1-1, another BBB carbohydrate transporter, in *Mfs3* and *pippin* null mutants, while RNAi-mediated knockdown is not compensated for. This means that the compensatory mechanisms in place upon mRNA degradation following RNA interference can be vastly different from those resulting from a null mutation.

Keywords: blood-brain barrier, carbohydrate transport, compensatory mechanisms, transporter regulation, transport dynamics

INTRODUCTION

To allow full functionality the brain requires a lot of energy. Most of the energy used in the nervous system is gained via carbohydrate metabolism. The human adult brain, despite accounting for only 2% of the bodies overall mass, consumes ~20% of the total oxygen (Mink et al., 1981; Laughlin et al., 1998; Harris et al., 2012). The oxygen is used to metabolize large amounts of glucose. The human brain uses about 90 g of glucose per day; during childhood carbohydrate usage is even higher (Kuzawa et al., 2014). Likewise, the blowfly retina consumes ~10% of the total ATP produced, which is close to the consumption observed in vertebrates (Laughlin et al., 1998).

Neuronal activity also relies on a tightly regulated extracellular milieu to allow signal conductance. Thus, the brain is shielded from potentially harmful substances, like high, and fluctuating ion concentrations found in circulation, by the blood-brain barrier (BBB). In mammals, the endothelial cells forming brain capillaries build intercellular tight junctions that prevent paracellular diffusion, thereby uncoupling the brain from circulation. In addition, efflux

transporters of the ABC family transport lipophilic, membrane-permeable molecules out of the BBB-forming cells to protect the nervous system from neurotoxic substances (for reviews see Löscher and Potschka, 2005; Koehn, 2020). To allow sufficient nutrient supply, a variety of transport proteins are expressed in the endothelial cells (for a review on metabolite transport at the BBB, see Weiler et al., 2017). In mammals, Glut1 is the main carbohydrate transporter found in the BBB-forming cells. Two differently glycosylated isoforms of Glut1 have been found in the mammalian nervous system, a 45 kDa and a 55 kDa isoform, that show identical transport kinetics (Birnbaum et al., 1986; Sivitz et al., 1989). The 55 kDa isoform is exclusively expressed in the endothelial cells and localizes to the luminal and abluminal membranes, while the 45 kDa isoform is found in astrocytes (Dick et al., 1984; Gerhart et al., 1989; Sivitz et al., 1989; Harik et al., 1990; Farrell and Pardridge, 1991; Maher et al., 1991, 1994; Simpson et al., 2001). In addition to Glut1, sodium glucose cotransporters (SGLTs) are expressed in the BBB upon stress. SGLT1 and SGLT2 have been shown to be expressed upon oxygen deprivation or ischemia, but seem to play a minor role in glucose uptake under normal conditions (Nishizaki et al., 1995; Nishizaki and Matsuoka, 1998; Elfeber et al., 2004; Enerson and Drewes, 2006; Vemula et al., 2009; Yu et al., 2013). Interestingly, the abundance of GLUT1 in the BBB seems to be regulated by hypoglycemia (Boado and Pardridge, 1993; Kumagai et al., 1995; Simpson et al., 1999). However, the regulatory mechanisms that underlie transporter regulation in the mammalian BBB are unknown.

In *Drosophila*, as in mammals, the brain is shielded from circulation. Here, the BBB is formed by two layers of glial cells, the subperineurial glial cells and the perineurial glial cells that surround the entire nervous system (reviewed in Limmer et al., 2014; Yildirim et al., 2019). Insects possess an open circulatory system, thus all organs, including the brain, are floating in the hemolymph. Therefore, the BBB surrounds the entire nervous system like a sheath. The subperineurial glial cells form intercellular pleated septate junctions that prevent paracellular diffusion (Stork et al., 2008). As in mammals, efflux transporters protect the nervous system from lipid-soluble toxic substances (reviewed in Hindle and Bainton, 2014). To ensure sufficient supply of nutrients and other essential substances to the nervous system a variety of solute carrier family transporter proteins are expressed in the BBB (Desalvo et al., 2014; Weiler et al., 2017). In addition, carbohydrate transporters are required to provide a sufficient supply of carbohydrates to the nervous system. As well as glucose, the non-reducing disaccharide trehalose is found in high quantities in circulation in *Drosophila* (Wyatt and Kalf, 1957; Lee and Park, 2004; Broughton et al., 2008; Pasco and Léopold, 2012). It has been shown that glucose can be readily taken up into the nervous system (Volkenhoff et al., 2018). Furthermore, the trehalose transporter 1-1 (Tret1-1) is expressed specifically in the perineurial glial cells of the *Drosophila* BBB (Volkenhoff et al., 2015). Tret1-1 is homologous to mammalian GLUT6 and GLUT8 and has been shown to transport trehalose and glucose (Kanamori et al., 2010; Hertenstein et al., 2020). How carbohydrates are taken up into the subperineurial glial cells of the BBB and the other neural cells

in the *Drosophila* nervous system is currently unknown. There are several homologs of mammalian GLUT1 encoded in the *Drosophila* genome: the closest homologs are dmGlut1, dmSut1 (sugar transporter 1), dmSut2, dmSut3, and CG7882. dmGlut1 is specifically expressed in neurons and may facilitate carbohydrate uptake there (Volkenhoff et al., 2018). Transcriptomic and *in situ* data for CG7882 and dmSut1-3, indicate very little or no expression in the nervous system, suggesting no major role in neural carbohydrate transport (Weizsmann et al., 2009; Croset et al., 2018; Davie et al., 2018).

Here, we identify two additional carbohydrate transporters expressed in the *Drosophila* BBB, Major Facilitator Superfamily Transporter 3 (MFS3, CG4726) and Pippin (CG4797). Pippin is expressed in both perineurial and subperineurial glial cells, while MFS3 is expressed in the perineurial glial cells only. Both transporters are able to facilitate uptake of glucose and trehalose when heterologously expressed in *Xenopus laevis* oocytes. Likewise, the simultaneous loss of Pippin and MFS3 in perineurial glia, and Pippin alone in subperineurial glia leads to decreased uptake of glucose. Interestingly, loss of either transporter or both transporters does not have any major phenotypic consequences. We demonstrate here that in null mutants compensatory upregulation of Tret1-1 rescues the detrimental effects of acute transporter loss on viability and carbohydrate transport at the BBB, while RNAi-mediated knockdown is not compensated for. In summary, we show that expression of carbohydrate transporters in the *Drosophila* BBB is highly dynamic and can be adapted to suboptimal circumstances like loss of one transporter. This dynamic adaptation of carbohydrate transport can most likely also be used to spare the nervous system from effects of hypoglycemia or malnutrition.

MATERIALS AND METHODS

Fly Stocks

Flies were kept at room temperature or 25°C. The following fly lines were used w^{-1} ;nrv2-Gal4;nrv2-Gal4, apontic-Gal4, mCherry^{dsRNA} (BL35785), UAS-CD8-GFP, nanos-Cas9^{attP2A} (BL36046) (Bloomington *Drosophila* stock center), *PBac{681.P.FSVS-1}MFS3^{CPT1002305}* (Kyoto stock center), pippin-dsRNA: w^{1118} ; P{GD4548}^{v10598} (VDRC), repo-Gal4; repo-Gal4, alrm-Gal4; alrm-Gal4, gli-Gal4 (Christian Klämbt), moody-Gal4 (Stork et al., 2008), 46F-Gal4 (Hummel et al., 2002), MFS^{dsRNA4726R-3} (Japanese National Institute of Genetics), UAS-FLII¹²Pglu-700 μ 86 (Volkenhoff et al., 2018). The dsRNA-constructs used in the RNAi screen are indicated in **Supplementary Table 1** and were obtained from Bloomington *Drosophila* stock center, VDRC or the National Institute of Genetics (NIG).

RNA Interference Screen

The RNAi screen was performed as follows: dsRNA lines were crossed to repo-Gal4; repo-Gal4 for panglial dsRNA expression. Crosses were kept at 25°C throughout development. After 2 weeks, viability of the offspring was determined and, if available, 20 female flies were selected, and locomotor capacity was tested in the island assay 1 week later (Schmidt et al., 2012).

RNA Interference Viability Assessment

pippin^{dsRNA10598} and *Mfs3*^{dsRNA4726R-3} were first crossed with a panglial driver (repo-Gal4; repo-Gal4). Crosses were performed at 25°C, after 2 weeks the viability of the offspring was determined. This method was repeated using glial subtype specific Gal4 drivers.

Analysis of Sugar Transport Capacity in *Xenopus laevis* Oocytes

Oocytes were isolated from female *Xenopus laevis* frogs as previously described (Becker et al., 2004; Becker, 2014). The procedure was approved by the Landesuntersuchungsamt Rheinland-Pfalz, Koblenz (23 177-07/A07-2-003 §6). *D. melanogaster pippin* and *Mfs3* were first cloned into a pUASTattBrfa3xHA vector (Rodrigues et al., 2012). Afterwards, the coding sequence with the C-terminal 3xHA-tag was cloned into a pGEM-He-Juel vector. cRNA was synthesized by *in vitro* transcription using the mMACHINE[®] T7 Kit (Fisher Scientific). Oocytes of the developmental stages V and VI were injected with 18–20 ng of cRNA. Measurements were conducted 3–6 days after injection. Expression of Pippin-3xHA and MFS3-3xHA on the surface of oocytes was confirmed by immunohistochemistry using an anti HA antibody (Covance).

82.5 mM NaCl, 2.5 mM KCl, 1 mM CaCl₂, 1 mM MgCl₂, 1 mM Na₂HPO₄, 5 mM HEPES. Transport capacity for trehalose, glucose and fructose was determined using ¹⁴C-labeled sugar in oocyte saline (82.5 mM NaCl, 2.5 mM KCl, 1 mM CaCl₂, 1 mM MgCl₂, 1 mM Na₂HPO₄, 5 mM HEPES, pH 7.2) at a concentration of 0.15 μCi/100 μl. ¹⁴C₁₂-trehalose was purchased from Hartmann Analytic, Braunschweig (#1249), ¹⁴C₆-glucose and ¹⁴C₆-fructose were purchased from Biotrend, Köln (#MC144-50 and 66 #MC1459-50). For each experiment 95 μl of sugar substrate was added to a batch of 6–8 oocytes and incubated for 60 min. Cells were washed four times with 4 ml of ice-cold oocyte saline. Individual cells were transferred to Pico Prais scintillation vials (Prekin Elmer) and lysed in 200 μl 5% SDS by shaking at 190 rpm for 30 min at 20–28°C. Three milliliters of Rotiszint[®] eco plus scintillation cocktail (Carl Roth) was added to each vial and scintillation was measured using a Tri-Carb 2810TR scintillation counter (Perkin Elmer).

Transport-mediated substrate uptake was determined by subtracting the uptake in native oocytes from the uptake in Pippin or Mfs3-expressing cells. Significance in difference was calculated using a one-tailed *T*-test or the Mann–Whitney-*U*-test for analysis of non-uniformly distributed samples.

Generation of CRISPR Mutants

Null mutants were generated using CRISPR-mediated homologous recombination. The sgRNA target sequences (*Mfs3*: sgRNA1: GGATATATAGGCCTTACTG, sgRNA2: A ATGAATTCGCTATTCAGGG; *pippin*: sgRNA1: GGTAGCA TATAGTAGGGG, sgRNA2: CGAGTCTAGGGCGACTAC G) were cloned into a pCFD3-dU6:3gRNA vector (Addgene). To generate the homology construct, the mini-white coding sequence flanked by homology arms (about 1.5 kb upstream and downstream of the coding sequence of either *Mfs3* or *pippin*) was cloned into a pCR-Blunt (ThermoFisher) backbone using Golden

Gate cloning (Engler et al., 2008) (primers to amplify homology regions from genomic DNA: *Mfs3*: upstream homology arm: CCACTGCAAATGGGGAAG and CTGCCGAATGCTAAT, downstream homology arm: CCCTGAATAGCGAATTCATG and GGTCGAAGTGCAGCGTCT; *pippin* upstream homology arm: TCAATGGCAAATGACG and CCTATTATCAAGGTG C, downstream homology arm: CGTAGTCGCCCTAGACTC and CCCAAAGCTCAACCAAC). The sgRNA vectors together with the homology construct were injected into nanos-Cas9^{attP2A} embryos to induce homologous recombination.

Generation of Pippin-HA Minigene

The gene locus (including 2.2 kb upstream and 0.5 kb downstream of the coding sequence) of *pippin* was assembled and C-terminally 3xHA-tagged using Golden Gate cloning (Engler et al., 2008). The assembled locus was inserted into a pUAST attB rfa vector (Stephan et al., 2008) using XbaI and HindIII restriction sites (thereby removing the UAS cassette). The resulting vector was integrated into the fly genome at landing site 86Fb.

Age Matching of Flies for Lifespan and Activity Monitoring

Flies of the desired genotype were placed in cages with an apple juice agar plate. After 24 h, plates were exchanged and left overnight. Embryos were washed from the plate with PBS and collected using a Pasteur pipette. Embryos were transferred into vials containing standard food. Vials were kept at 18°C for 3 weeks and adult females were collected.

Survival Analysis

Female flies were kept in batches of 20 at 25°C throughout the experiment. Flies were flipped three times a week onto fresh food, deaths were counted. Survival rates were determined using the Kaplan-Meier approach. *P*-values were calculated using Log Rank test.

Analysis of Locomotive Activity (DAM)

Female flies were sorted into vials of 20 and aged at 25°C for 2 or 5 weeks. Single flies were sorted into tubes containing standard food and loaded into a *Drosophila* activity monitor (DAM). Monitors were placed in an incubator with a 12-h light dark cycle and activity was recorded. The activity over 24 h was determined by the number of beam crosses made by the animal in this time period. *P*-values for significance were determined using Mann–Whitney rank sum test.

Analysis of Escape Response (RING Assay)

Female flies were kept in batches of 20 and aged at 25°C for 2 or 5 weeks. Flies were transferred into negative geotaxis tubes and loaded into the RING apparatus in groups of 10 (Gargano et al., 2005). Tubes were dropped from a height of 30 cm to initiate climbing response. This was repeated five times with a 30 s break between drops to allow flies to recover. The position of the flies in the tubes was captured in digital images and the mean velocity of the flies was determined. *P*-values for significance were determined using Mann–Whitney rank sum test.

Analysis of Circulating Glucose Levels (Glucose GO kit)

Fifteen adult female flies were collected, and a puncture was made in the thorax of each fly using forceps. Flies were then transferred to a 0.5 ml tube (containing a small hole in the base) that was placed in a 1.5 ml Eppendorf tube. Tubes were centrifuged at 13,000 RPM for 5 min at 4°C. The supernatant was collected and transferred to a new Eppendorf tube. Hemolymph was heat-inactivated at 80°C for 10 min to abolish endogenous enzymatic activity, cooled and 25 µl of buffer A (5mM Tris-HCL (pH 6.6), 137 mM NaCl, 2.7 mM KCL) was added. Glucose levels were determined using a Glucose (GO) assay kit (Sigma-Aldrich) according to the manufacturer's instructions. Difference between the control and null mutants was assessed using a one-tailed *t*-test.

Immunohistochemistry

Wandering third instar (L3) larval or adult brains were dissected and stained following standard protocols. Samples were imaged using a Zeiss LSM 880 (Zeiss, Oberkochen, Germany). The following antibodies were used: guinea pig anti-Tret1-1 PA (1:50, Volkenhoff et al., 2015), mouse anti-NC120 (1:2 Hybridoma), rabbit anti-laminin gamma (1:1,000 Abcam A47651), Chicken anti-GFP (1:500, Aves Labs), mouse anti-HA (1:1,000 Covance). Tret1-1 fluorescence was determined by comparing the mean gray values of Tret1-1 staining of null mutants or knockdown animals to the respective control. *N* is the number of independent experiments; *n* is the total number of animals analyzed.

Measurement of Glucose Uptake (FRET)

Null mutants or dsRNA lines were crossed with flies expressing *UAS-FLII¹²Pglu-700µ86* FRET glucose sensor under the control of either apt-Gal4 or moody-Gal4. Larval brains of the desired genotype were dissected in HL3 buffer (70 mM NaCl, 5 mM KCl, 20 mM MgCl₂, 10 mM NaHCO₃, 115 mM sucrose, 5 mM trehalose, 5 mM HEPES; pH 7.2; ca. 350 mOsm) and attached to Poly-D-Lysine-coated coverslips. Samples were then mounted in a custom-made flow through chamber and secured to a Zeiss LSM 880 (Zeiss, Oberkochen, Germany). Buffer exchange was facilitated using a mini-peristaltic pump (MPII, Harvard Apparatus). Fluorescent images were captured using a 20x/1.0 DIC M27 75mm emersion objective (Zeiss, Oberkochen, Germany) directly after dissection. An excitation of 436/25 nm, beam splitter 455 nm, emission 480/40 nm (CFP channel); excitation 436/25 nm, beam splitter 455 nm, emission 535/30 nm (YFP channel) was used. Each brain was imaged in an independent experiment (*n* = 8–12). After 2.5 min HL3 buffer was replaced with 10 mM glucose buffer (HL3 supplemented with glucose; pH 7.2) then exchanged back to HL3 after 9 min. Data analysis was performed by generating a ROI containing the larval brain and calculating the mean gray value, minus background. *N* is the number of independent experiments; *n* is the total number of animals analyzed. Statistical regression and analysis was carried out using SigmaPlot software (Jandel). The rate of glucose uptake was calculated by selecting 10 consecutive timepoints at the beginning of the slope. The volume of glucose entering the cell was determined by the mean difference between the baseline and the maximum plateau (10 mM glucose). Statistical

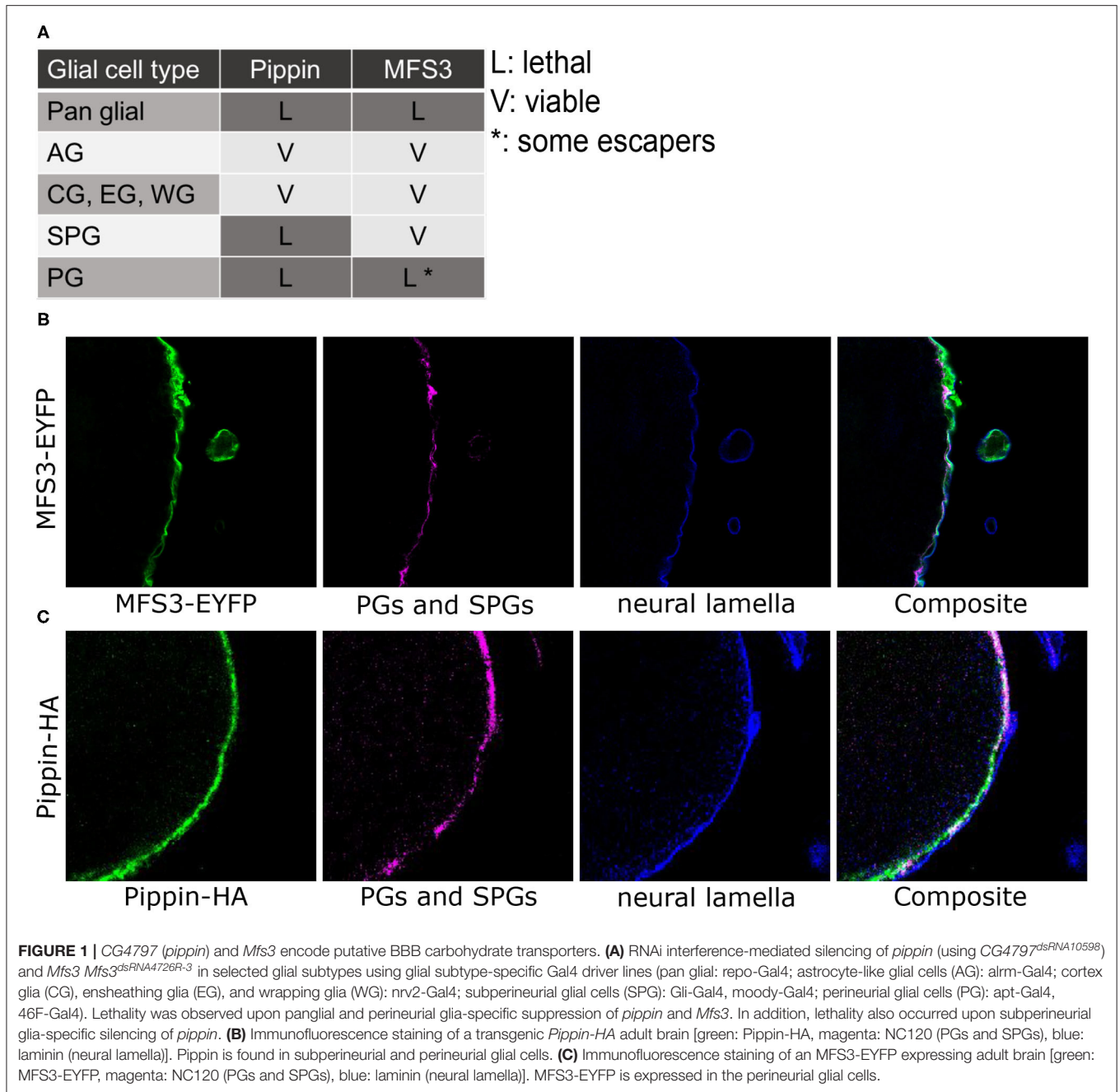
differences were calculated using a Mann–Whitney Rank Sum test (pairs). *P* < 0.05 were considered as significant.

RESULTS

CG4797 (Pippin) and Mfs3 Encode Putative Carbohydrate Transporters of the BBB

Previously, we showed that all cell types of the *Drosophila* nervous system are capable of taking up glucose (Volkenhoff et al., 2018). Since carbohydrates are hydrophilic molecules, they cannot diffuse over the plasma membrane and thus need to be transported. The only two carbohydrate transporters identified in the *Drosophila* CNS by now, Tret1-1 and Glut1, however, are expressed in the perineurial glial cells or the neurons, respectively. Thus, we set out to identify additional carbohydrate transporters expressed in the *Drosophila* nervous system. To this end we performed a small, biased RNA interference-based screen, in which we knocked down putative carbohydrate transporters encoded in the *Drosophila* genome specifically in the glial cells [genes with a predicted sugar transport function according to protein domain annotations from InterPro (<http://www.ebi.ac.uk/interpro/>) and UniProt (<http://www.uniprot.org/>), **Supplementary Table 1**]. This screen identified 14 putative carbohydrate transporters required in glial cells, amongst them CG4797 (Pippin) and Major Facilitator Superfamily Transporter 3 (MFS3, CG4762) (**Supplementary Table 1**). We focused our efforts on these two genes. Knockdown of the two genes specifically in glial cells using RNA interference (*pippin*^{dsRNA10598}, *MFS3*^{dsRNA4726R-3}) leads to pupal lethality, indicating a function in glial cells (**Figure 1A**). *Drosophila* MFS3 shows 35% identity to the mouse anion/cation symporter (ACS) Sialin (NCBI protein blast), but the ACS consensus sequence is not fully conserved, indicating that MFS3 does not encode an ACS (Laridon et al., 2008). CG4797 encodes an SLC2 family glucose transporter most homologous to mouse GLUT6 and GLUT8 (NCBI protein blast). This indicates that CG4797 encodes a carbohydrate transporter; thus, we named the gene *pippin*, after Frodo's friend, whose biggest concern is usually where to get the next meal.

To identify the glial subtype in which the putative transporters are needed, we repeated the knockdown experiments using glial subtype drivers (*nrv2-Gal4*: cortex glia, ensheathing glia and wrapping glia; *almr-Gal4*: astrocyte-like glial cells; *Gli-Gal4* or *moody-Gal4*: subperineurial glial cells; *apt-Gal4* or *46F-Gal4*: perineurial glial cells). Knockdown of *pippin* in perineurial or subperineurial glial cells led to lethality, while knockdown in any other glial subtype had no phenotypic consequences (**Figure 1A**). In contrast, knockdown of *Mfs3* only led to lethality in perineurial glial cells (**Figure 1A**). This indicates that Pippin is needed in both BBB-forming glial cells, while MFS3 is just essential in the perineurial glial cells. To verify the expression, we took advantage of an existing EYFP protein trap for MFS3 (MFS3^{CPT1002305}). MFS3-EYFP localizes to the perineurial glial cells as seen when co-stained with NC120 (subperineurial glial cells) and laminin (neural lamella) (**Figure 1B**), as suggested from the knockdown experiments. To analyze the localization of *pippin*, we cloned the complete *pippin* locus, including upstream and

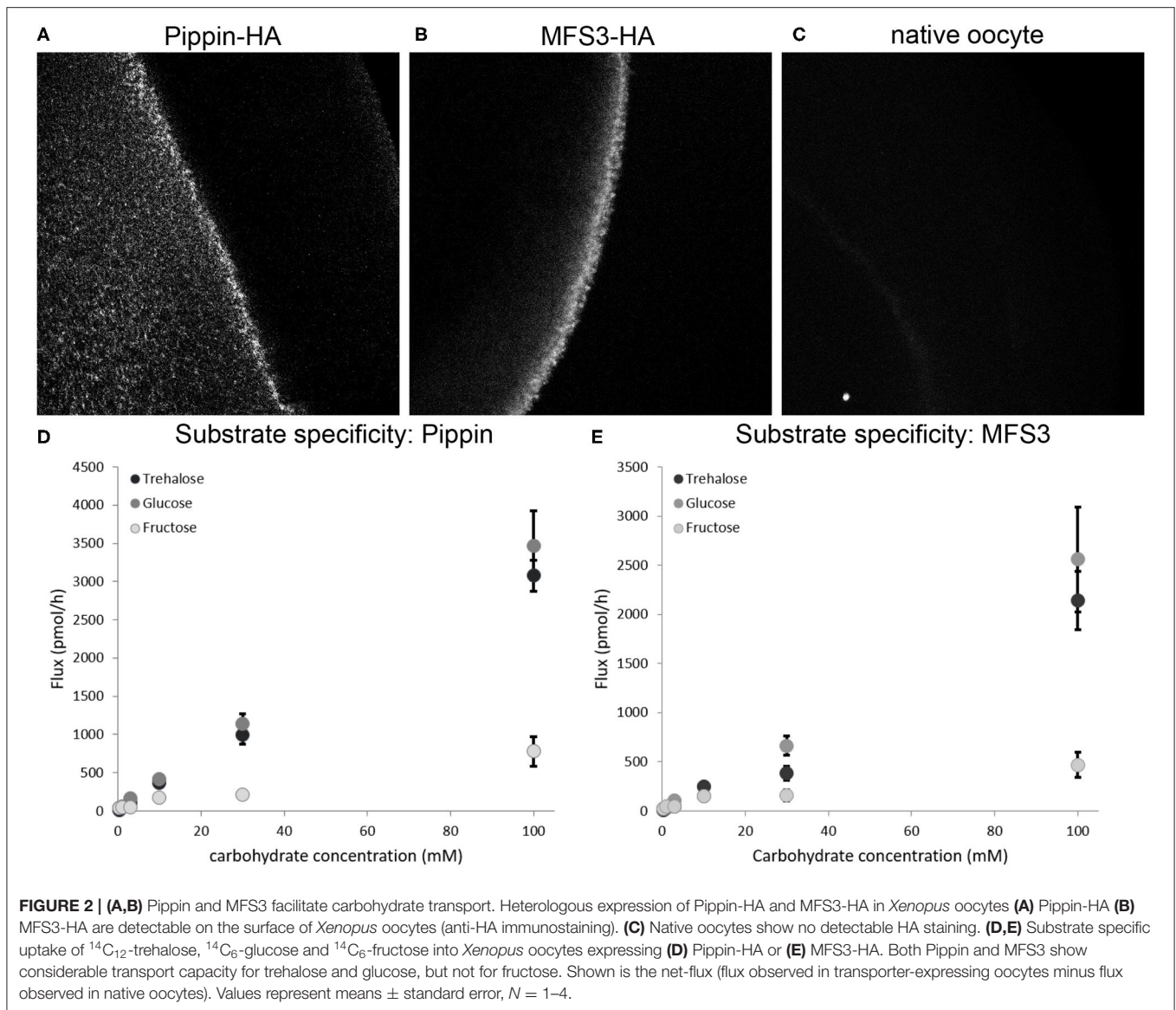


downstream regions to include all regulatory elements, and fused a C-terminal 3xHA-tag to the coding sequence. Flies carrying this *pippin* minigene construct, show Pippin-HA expression in the perineurial and subperineurial glial cells as assumed from the RNAi-experiments (Figure 1C).

Pippin and MFS3 Facilitate Carbohydrate Transport

To analyze whether the two newly identified BBB transporters are indeed able to facilitate carbohydrate uptake into the perineurial and/or subperineurial glial cells, we expressed *Drosophila* Pippin

and MFS3 in *X. laevis* oocytes. To verify expression of the transporters we tagged Pippin and MFS3 with a 3xHA-tag. Both Pippin-HA and MFS3-HA are produced in *Xenopus* oocytes upon mRNA injection and localize to the membrane (Figures 2A–C). To analyze whether the transporters facilitate uptake of carbohydrates found in the *Drosophila* hemolymph, we incubated the respective oocytes with different concentrations of ¹⁴C-labeled glucose, trehalose, or fructose (Figures 2D,E). Interestingly, both Pippin and MFS3 facilitate uptake of glucose and trehalose efficiently (Figures 2D,E). Fructose, however, is transported at a much lower rate. Since naturally occurring



fructose concentrations in the larva seem to be rather low compared to glucose and trehalose concentrations, it is unlikely that this transport is of physiological relevance (Mishra et al., 2013). These experiments show that the newly identified BBB transporters are indeed carbohydrate transporters. Fitting of the data, shown in **Figures 2D,E**, did not result in reliable K_m or V_{max} values. Therefore, more experiments need be carried out to analyze the transport kinetics of Pippin and MFS3 in *Xenopus* oocytes.

Pippin and MFS3 Null Mutants Are Viable, but Display Shortened Lifespan and Reduced Locomotor Activity

To further analyze the consequences of loss of Pippin or MFS3, we generated null mutants for both transporters. We

used CRISPR-mediated recombination to replace the entire coding sequence of *pippin* or *Mfs3* with a mini-white, thereby creating null mutants (**Supplementary Figure 1**). Interestingly, both *pippin*^{-/-} and *Mfs3*^{-/-} null mutants are viable and fertile, which contrasts with the phenotype observed upon glia-specific knockdown using RNA interference.

To assess viability of the mutants, we performed lifespan experiments. Indeed, *pippin*^{-/-} and *Mfs3*^{-/-} null mutants are short-lived compared to control animals (**Figure 3A**). Thus, we analyzed their phenotype in more detail. We assessed the activity of the null mutants after 2 and 5 weeks of age (**Figures 3B,C**). Already at the age of 2 weeks, both *pippin*^{-/-} and *Mfs3*^{-/-} null mutants are less active than control animals. To distinguish between a reduction in activity to save energy and the incapacity to move, we in addition studied the animals' escape response at the age of 2 and 5 weeks using a rapid iterative negative geotaxis

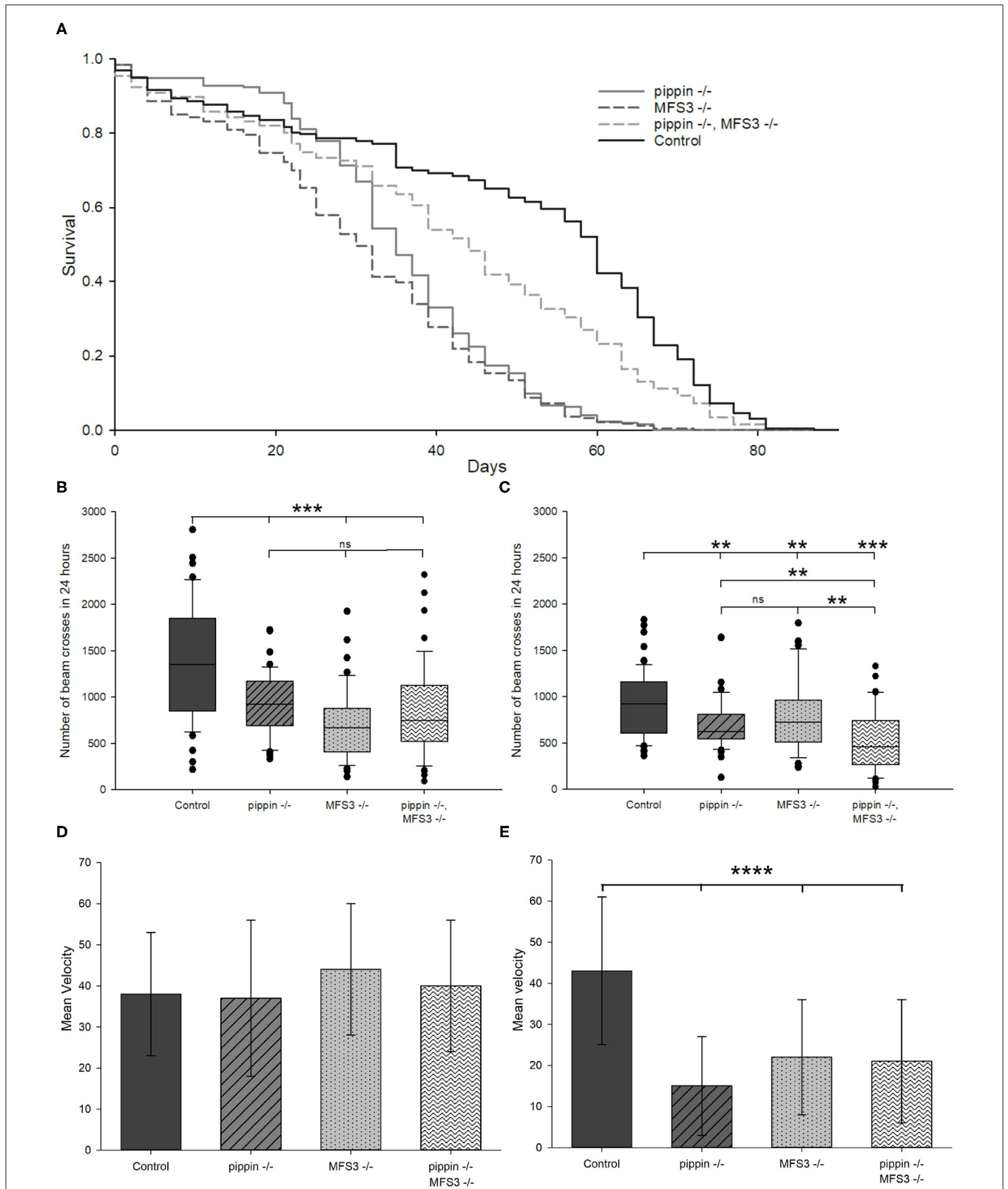


FIGURE 3 | *pippin* and *Mfs3* null mutants are viable, but display shortened lifespan and reduced locomotor activity. **(A)** Survival curves of null mutants and control animals. All mutants show a reduced lifespan compared to control animals, however double *pippin*^{-/-}; *Mfs3*^{-/-} mutants live significantly longer than single mutants. (Continued)

FIGURE 3 | $N = 3$, $n \geq 180$ ($pippin^{-/-}$: $p < 10^{-21}$, $Mfs3^{-/-}$: $p < 10^{-23}$, $pippin^{-/-}$, $Mfs3^{-/-}$: $p < 10^{-4}$; log-rank test). **(B,C)** Activity monitored over 24 h of null mutants and control animals at 2 weeks old **(B)** and 5 weeks **(C)** of age. All mutants show a reduction in activity compared to control animals at 2 weeks of age, however the double mutants show a progressive reduction in activity moving significantly less than the single mutant at 5 weeks of age. $N = 3$; $n \geq 58$; ** $p \leq 0.01$, *** $p \leq 0.001$. **(D,E)** Negative geotaxis assay measuring climbing ability as an escape response of 2 **(D)** and 5 **(E)** weeks old flies. Single $pippin^{-/-}$ or $Mfs3^{-/-}$ mutants show no reduction in climbing ability at 2 weeks but show a decrease in activity at 5 weeks of age. $N = 5$; $n \geq 500$; **** $p \leq 0.0001$.

(RING) assay (Gargano et al., 2005), in which the flies are put in vials that are tapped on the table. This tapping induces an escape response, where the flies run up the walls of the vial. Depending on their locomotor capabilities the animals climb the walls faster or slower (**Figures 3D,E**). At the age of 2 weeks all genotypes are capable of a fast escape response (**Figure 3D**). Thus, at this age, the animals are able to move as well as control flies, but are nevertheless less active, most likely as a means of saving energy. However, at the age of 5 weeks the velocity of $pippin^{-/-}$ and $Mfs3^{-/-}$ null mutants is significantly reduced, indicating progressive loss of locomotor abilities (**Figure 3E**).

Since RNAi-mediated knockdown of *pippin* or *Mfs3* are pupal lethal, but the null mutants are not, we checked for putative compensation of the loss of either transporter. To this end, we created double $pippin^{-/-}$, $Mfs3^{-/-}$ mutants and analyzed their phenotype. Interestingly, $pippin^{-/-}$, $Mfs3^{-/-}$ double mutants are also viable and fertile. Surprisingly, lifespan experiments show that the double mutants live longer than the respective single mutants, albeit not as long as control animals (**Figure 3A**). To establish whether the double mutants move even less than the single mutants to save energy, we analyzed their activity at 2 and 5 weeks of age (**Figures 3B,C**). At 2 weeks of age the double mutant is significantly less active than wildtype control animals but moves as much as either single mutant (**Figure 3B**). In contrast, at the age of 5 weeks, the double mutant animals are significantly less active than either single mutant (**Figure 3C**). To distinguish between an inability to move and an energy-saving reduction of activity, we also analyzed the escape response. Here, the double mutant animals are indistinguishable from single mutant animals at either time point (**Figures 3D,E**). This indicates that the double mutant animals have the ability to move as well as the single mutants. However, they seem to move progressively less over their lifespan, probably to save energy.

Compensatory Increase in Circulating Carbohydrate Levels and Upregulation of Tret1-1 Upon Loss of Pippin or MFS3

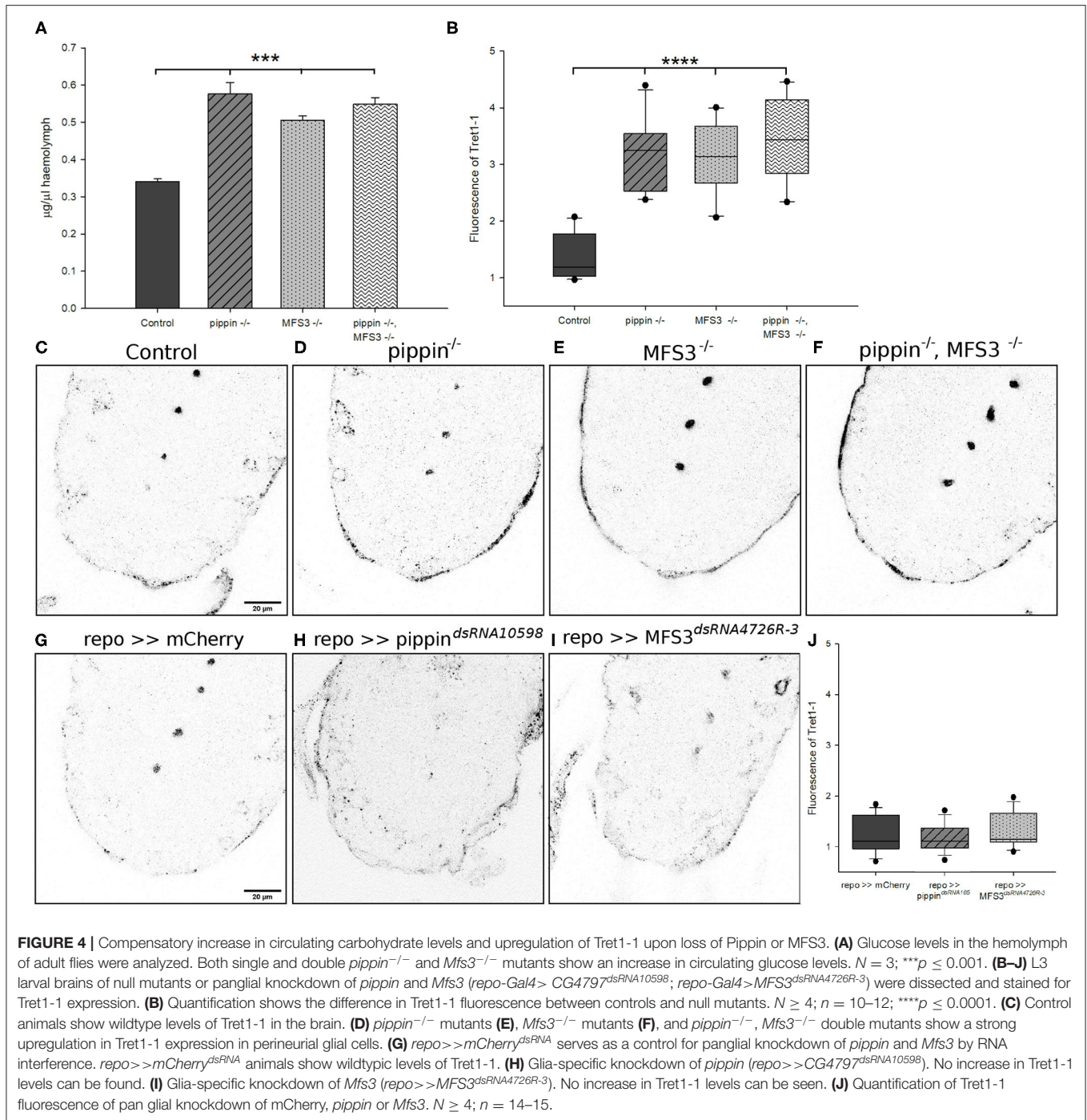
To understand why $pippin^{-/-}$ and $Mfs3^{-/-}$ null mutants are viable, while glia-specific acute knockdown is lethal, we investigated other possible compensatory mechanisms. Classic carbohydrate transporters, like SLC2 family carbohydrate transporters, are facilitative transporters, which means that they allow uptake of the respective carbohydrate into a cell driven by a concentration gradient. Thus, an increase in the concentration gradient between the extracellular milieu and the cytosol of the respective cell, accelerates carbohydrate uptake into the cell. Therefore, we analyzed circulating glucose levels in $pippin^{-/-}$ and $Mfs3^{-/-}$ null mutants to see if deficits in transporter expression might be compensated by elevated circulating sugar

levels (**Figure 4A**). Indeed, $pippin^{-/-}$ and $Mfs3^{-/-}$ null mutants, as well as the double mutants display elevated hemolymph glucose levels that might facilitate glucose uptake into the brain.

An alternative mode of compensation for the loss of a carbohydrate transporter would be to upregulate an alternative transporter. The only other carbohydrate transporter known to be expressed in the Drosophila BBB, besides Pippin and MFS3, is Tret1-1 (Volkenhoff et al., 2015). As Pippin and MFS3, Tret1-1 facilitates uptake of glucose and trehalose when heterologously expressed in *Xenopus* oocytes (Kanamori et al., 2010; Hertenstein et al., 2020). To assess if Tret1-1 could compensate for the loss of either Pippin or MFS3 in the null mutants, we stained null mutant L3 brains for Tret1-1 expression in the perineurial glial cells. Interestingly, Tret1-1 expression is strongly increased in the perineurial glial cells of $pippin^{-/-}$ and $Mfs3^{-/-}$ null mutants as well as $pippin^{-/-}$, $Mfs3^{-/-}$ double mutants (**Figures 4B–F**). The increase in Tret1-1 expression is not significantly higher in the double mutants than in the single mutants. Loss of Pippin, however, does not induce compensatory misexpression of Tret1-1 in the subperineurial glial cells (**Supplementary Figure 2**). This increase in Tret1-1 expression in the perineurial glial cells could compensate for a reduction of carbohydrate uptake caused by loss of Pippin and/or MFS3. To understand the difference between RNAi-mediated knockdown of *pippin* and *Mfs3* and the null mutants, we also analyzed Tret1-1 expression in animals with a glia-specific knockdown of either *pippin* or *Mfs3* (**Figures 4G–J**). Indeed, glia-specific knockdown of *pippin* or *Mfs3* does not induce a compensatory upregulation of Tret1-1, potentially explaining the phenotypic differences (**Figures 4G–J**). These findings suggest that null mutations, like a complete loss of the coding region as in the case of our $pippin^{-/-}$ and $Mfs3^{-/-}$ mutants, induce different compensatory mechanisms than constant degradation of the respective mRNAs, as induced by RNA interference. If such differences in compensation are common, this could explain the discrepancies often found between RNAi-mediated knockdown phenotypes and null mutant phenotypes.

Pippin and MFS3 Facilitate Glucose Uptake in the Drosophila BBB

To study if loss of any of the described carbohydrate transporters has an effect on carbohydrate uptake into the BBB-forming glial cells, we analyzed glucose uptake into the respective cells using a genetically-encoded Förster resonance energy transfer (FRET)-based glucose sensor, FLII12Pglu-700 μ 86 (Fehr et al., 2003; Takanaga et al., 2008; Volkenhoff et al., 2018). This sensor allows visualizing carbohydrate uptake in living *ex vivo* L3 larval brains (Volkenhoff et al., 2018). To understand the changes in carbohydrate uptake in the different mutants and



knockdown animals, we expressed the glucose sensor either in the perineurial or subperineurial glial cells of the animals and analyzed glucose uptake capacity (Figures 5, 6). When we analyzed glucose uptake into the perineurial glial cells of animals with a perineurial glia-specific knockdown of *pippin* (using apt-Gal4), we found that the maximum concentration of glucose found in the cells is significantly reduced compared to that found in control animals (expressing mCherry-dsRNA) (Figures 5A,D). This indicates that Pippin indeed acts as a

carbohydrate transporter in the perineurial glial cells and that loss of Pippin reduces glucose uptake efficiency significantly. Interestingly, the initial glucose uptake rate does not change (Figure 5C). Since Pippin is also expressed in the subperineurial glial cells, we also analyzed glucose uptake into those cells. In this case, we expressed the dsRNA-construct as well as the glucose sensor using moody-Gal4. As expected upon loss of a carbohydrate transporter, both the glucose uptake rate as well as the maximal glucose concentration reached in the cells are

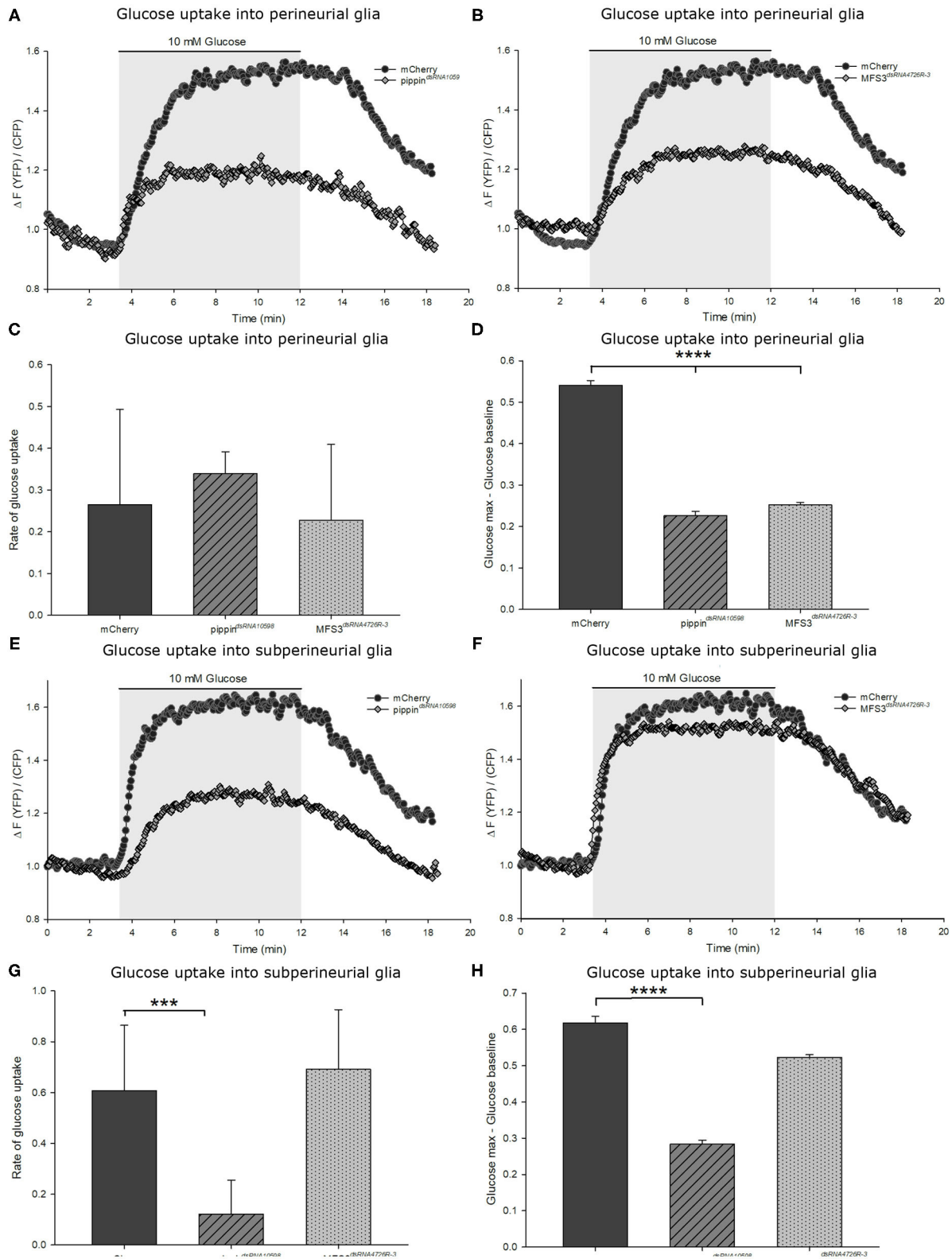


FIGURE 5 | Pipin and MFS3 facilitate glucose uptake into the Drosophila BBB-forming cells. Glucose uptake was measured in *ex vivo* L3 larval brains expressing a genetically encoded glucose sensor (FLII¹²Pglu-700 μ δ 6). **(A,B)** Example traces of brains with a perineurial knockdown of *pipin* (*apt-Gal4*>*pipin*^{dsRNA10598}) **(A)** or *MFS3* (*apt-Gal4*>*MFS3*^{dsRNA47269-3}) **(B)**. **(C,D)** Summary of glucose uptake rates and maximum change from baseline for perineurial glia. **(E,F)** Example traces of brains with a subperineurial knockdown of *pipin* (*sub-Gal4*>*pipin*^{dsRNA10598}) **(E)** or *MFS3* (*sub-Gal4*>*MFS3*^{dsRNA47269-3}) **(F)**. **(G,H)** Summary of glucose uptake rates and maximum change from baseline for subperineurial glia. Significance: *** p < 0.001, **** p < 0.0001.

(Continued)

FIGURE 5 | *Mfs3* (*apt-Gal4>MFS3^{dsRNA4726R-3}*) (**B**), where the glucose sensor is expressed in the perineurial glial cells. (**C**) Quantification of the rate of glucose uptake. The glucose uptake rate as calculated by the steepness of the slope shows no difference between transporter knockdown and control brains. (**D**) Quantification of the maximum glucose concentration in the cells. Shown is the difference between the maximum glucose concentration and the baseline glucose concentration. $N = 8-12$; **** $p \leq 0.0001$. (**E-H**) Glucose uptake into the subperineurial glial cells. (**E**) *moody-gal4>pippin^{dsRNA10598}* brains show a reduction in the uptake rate and overall levels of glucose entering the subperineurial glia. (**F**) *moody-Gal4>Mfs3^{dsRNA4726R-3}* brains show no difference in glucose uptake rate or maximum glucose levels. (**G,H**) Quantification of the glucose uptake rate and the maximum glucose concentrations reached in the subperineurial glial cells. (**G**) Rate of glucose uptake into the subperineurial glial cells in brains of the different genotypes (subperineurial glial knockdown). Knockdown of *pippin* in the subperineurial glial cells severely reduces glucose uptake rates. (**H**) Maximum glucose levels in subperineurial glial cells expressing *FLII¹²Pglu-700 μ .86*. Brains in which *pippin* is knocked down in the subperineurial glial cells show a lower maximum glucose level than control brains or *Mfs3* knockdown brains. $n = 8-12$; *** $p \leq 0.001$, **** $p \leq 0.0001$. Error bars show standard deviation.

significantly decreased upon loss of Pippin in the subperineurial glial cells (**Figures 5E-H**). Upon RNAi-mediated loss of MFS3, glucose transport is impaired in the perineurial glial cells, but not in the subperineurial glial cells (**Figures 5B-D,F-H**). This fits the expression of MFS3 in the perineurial but not in the subperineurial glial cells and suggests that, indeed, also MFS3 is essential for glucose transport into the perineurial glial cells.

Compensatory Upregulation Rescues Deficits in Carbohydrate Uptake Caused by Loss of Pippin and MFS3

To analyze if compensatory upregulation of *Tret1-1* can rescue glucose uptake efficiency in the *Drosophila* BBB, we analyze glucose uptake into the perineurial and subperineurial glial cells in *pippin^{-/-}* and *Mfs3^{-/-}* null mutant animals. *pippin^{-/-}* and *Mfs3^{-/-}* null mutant animals display wild type glucose uptake into the perineurial glial cells (**Figures 6A-D**). Thus, compensatory upregulation of *Tret1-1* indeed rescues deficits in carbohydrate transport. As expected, glucose uptake into the subperineurial glial cells is indistinguishable from controls in *Mfs3^{-/-}* null mutant animals (**Figure 6G**). In contrast, *pippin^{-/-}* mutant animals show reduced glucose uptake efficiency into the subperineurial glial cells, indicating a lack of compensation in this cell type (**Figures 6F-J**). These results match the expectations, since MFS3 is not expressed in the subperineurial glial cells and subperineurial loss of Pippin is not compensated for by *Tret1-1* upregulation.

We also analyzed carbohydrate uptake into the perineurial and subperineurial glial cells of *pippin^{-/-}*, *Mfs3^{-/-}* double mutants. Here, we find reduced uptake efficiency in both the perineurial and subperineurial glial cells (**Figures 6C,D,H-J**). The reduction of glucose uptake into the subperineurial glial cells most likely phenocopies the reduction found in *pippin^{-/-}* null mutants, since Pippin is the only transporter expressed in those cells. Interestingly, *Tret1-1* upregulation does not seem to be sufficient to rescue glucose transport deficits caused by loss of both Pippin and MFS3 in the perineurial glial cells (**Figures 6C,D**). This finding might explain the differences in lifespan and activity between the single and the double mutant animals.

DISCUSSION

Sufficient nutrient supply to the nervous system is essential for its proper function. Since the main energy source of the

brain is sugar, adequate carbohydrate transport over the BBB needs to be ensured. Thus, the vertebrate as well as the insect BBB-forming cells express carbohydrate transporters to facilitate uptake of sugars (Weiler et al., 2017). We report the identification of two additional carbohydrate transporters expressed by the BBB-forming glial cells of *Drosophila*, Pippin, and MFS3. Both transporters can facilitate uptake of glucose and trehalose (**Figure 2**). RNAi-mediated knockdown of either gene induces pupal lethality, while null mutants are viable and fertile. This discrepancy is found since null mutants show a compensatory upregulation of the carbohydrate transporter *Tret1-1*. Interestingly, such upregulation cannot be seen in knockdown animals, suggesting that there is a major difference in compensation if the mRNA of a certain gene is produced and then degraded or if there is no mRNA production since the coding sequence has been deleted. Similar discrepancies have been found comparing morpholino-induced knockdown phenotypes vs. mutant phenotypes in zebrafish or siRNA-mediated knockdown phenotypes vs. mutant phenotypes in mice (De Souza et al., 2006; Daude and Westaway, 2012; Kok et al., 2015; Rossi et al., 2015). In zebrafish, for example, *Egfl7* null mutants show compensatory upregulation of *Emilin* genes that rescue *Egfl7* loss. Such upregulation is not found in morpholino-knockdowns that thus show a severe vascular defects (Rossi et al., 2015). Interestingly, such compensation might even be conserved in humans. On Iceland individuals with a homozygous loss of *Egfl7* were identified, who do not suffer from any symptoms (Sulem et al., 2015). However, the underlying regulatory mechanisms are currently unknown. They are likely to be complex and will probably require much effort to unravel. In any case, such conserved differential compensation should be considered when studying the effects of gene knockdown and null mutations.

The data reported here shows that transporter expression at the BBB can be adapted to suboptimal circumstances, like in this case loss of one transporter. There are two potential mechanisms that could compensate for transporter loss: increase of the concentration gradient at the plasma membrane (circulation vs. cytosol), and compensatory upregulation of another transporter. In case of our null mutant flies we see compensation via both possibilities (**Figure 4**). The animals display higher circulating sugar concentrations that most likely increase the concentration gradient over the plasma membrane and thus make carbohydrate transport via facilitative transporters more efficient, as well as an upregulation of another transporter, *Tret1-1*. These compensatory mechanisms rescue transport

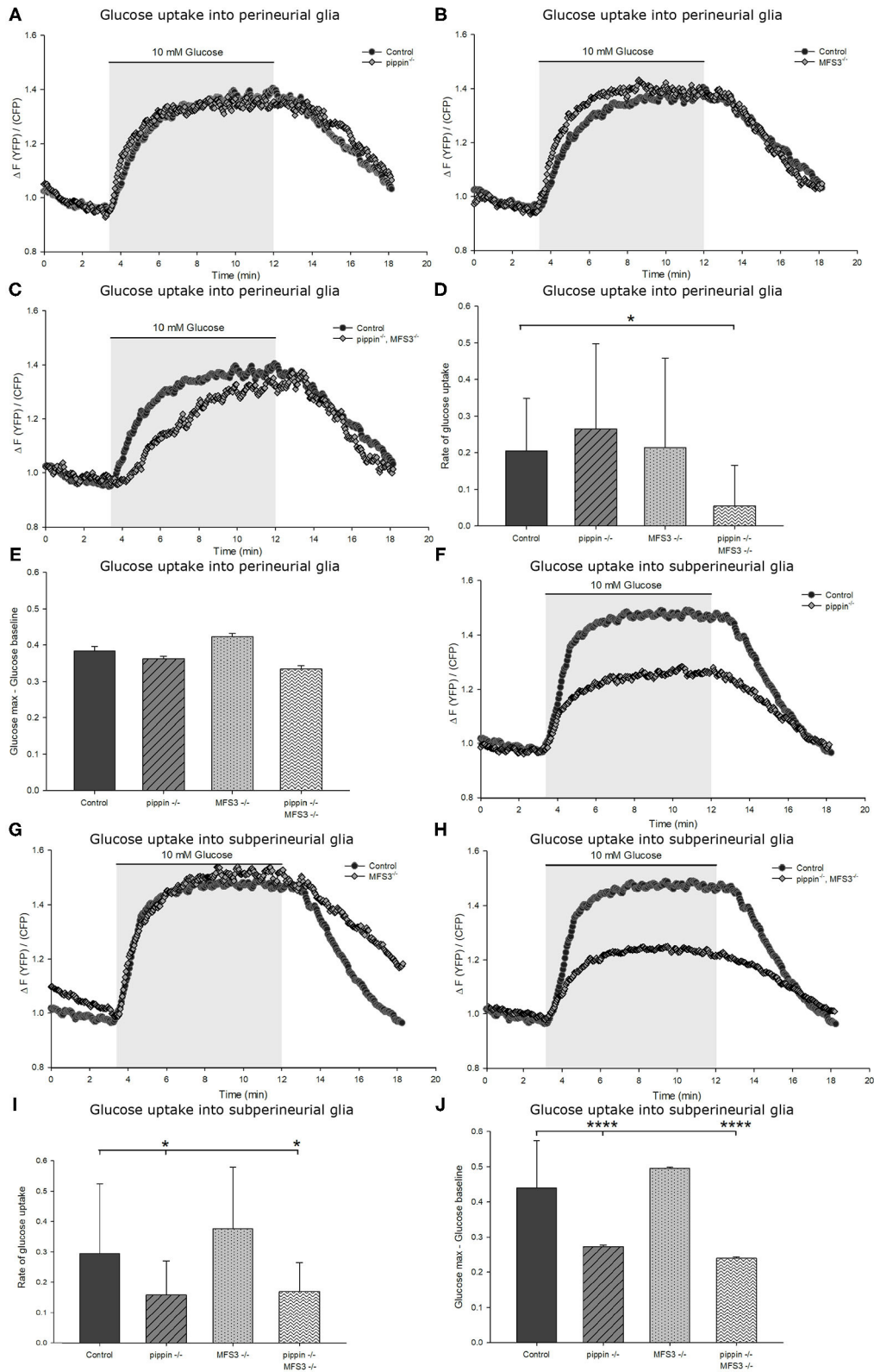


FIGURE 6 | Compensatory upregulation rescues deficits in carbohydrate uptake caused by loss of Pippin and MFS3. **(A–E)** Capacity of glucose uptake in *ex vivo* larval brains of *pippin*^{-/-} or *Mfs3*^{-/-} null single or double mutants expressing FLII¹²Pglu-700 μ . δ 6 in the perineurial glial cells. There is no difference observed in (Continued)

FIGURE 6 | glucose uptake rate or maximum glucose concentration compared to control brains for *pippin*^{-/-} (A) or *Mfs3*^{-/-} (B) single mutants. However, the double mutant (C) perineurial glial cells take up glucose significantly slower than single mutants or wildtype controls. (D) Quantification of the glucose uptake rate into perineurial glial cells in the indicated genotypes. The double mutant perineurial glial cells take up glucose significantly slower than single mutants or wildtype controls. *n* = 8–12; **p* ≤ 0.05. (E) Quantification of the difference between maximum glucose concentration and baseline glucose concentration. There is no observable difference between the genotypes. *n* = 8–12. (F–J) Glucose uptake and maximum glucose level in the subperineurial glial cells. (F) *pippin*^{-/-} mutant brains, but not *Mfs3*^{-/-} mutant brains (G) show reduced glucose uptake into the subperineurial glial cells. (H) *pippin*^{-/-}, *MFS3*^{-/-} double mutant brains show the same phenotype as *pippin*^{-/-} single mutant brains. Both the rate of glucose uptake (I) and the maximum glucose concentration (J) are reduced in both *pippin*^{-/-} single and *pippin*^{-/-}, *MFS3*^{-/-} double mutant brains. *n* = 8–12; **p* ≤ 0.05, *****p* ≤ 0.0001. Error bars show standard deviation.

efficiency as seen using a genetically encoded glucose sensor to assess glucose uptake properties (Figure 6). The increase in circulating carbohydrates suggests a crosstalk between the nervous system, probably the BBB-forming glial cells, and the periphery to regulate nutrient mobilization most likely from the fat body. That BBB transport defects can regulate systemic metabolism is a very interesting finding that will foster exciting follow up studies to unravel the regulatory mechanisms.

It has been shown previously that *Tret1-1* is upregulated upon starvation-induced hypoglycemia (Hertenstein et al., 2020). Together with the data reported here, this suggests that any alteration that leads to insufficient carbohydrate uptake results in compensatory upregulation of transport proteins, most likely to ensure sufficient energy provision to the nervous system. In the case of starvation, *Tret1-1* is upregulated via TGF- β signaling (Hertenstein et al., 2020). Since this signaling seems to be induced by hypoglycemia, it is very unlikely that TGF- β signaling is also regulating compensatory upregulation in the case of transporter loss (Hertenstein et al., 2020). Mammalian GLUT1 and SGLT1 and 2 have also been shown to be dynamically upregulated upon hypoglycemia or other insults like oxygen and glucose deprivation as a result of ischemia (Boado and Pardridge, 1993; Kumagai et al., 1995; Nishizaki et al., 1995; Nishizaki and Matsuoka, 1998; Simpson et al., 1999, reviewed in Elfeber et al., 2004; Enerson and Drewes, 2006; Vemula et al., 2009; Yu et al., 2013; Patching, 2016; Rehni and Dave, 2018). Thus, it is very likely that a flexible and dynamic regulation of carbohydrate transporters is an evolutionary conserved mechanism that ensures proper nervous system function even under suboptimal conditions. Since aberrations in carbohydrate availability and transport are thought to be a major cause of severe illnesses, like GLUT1 deficiency syndrome, Alzheimer's disease or epilepsy (Kapogiannis and Mattson, 2011; Arsov et al., 2012; Hoffmann et al., 2013; Koepsell, 2020), it will be very interesting to unravel the regulatory mechanisms that can lead to a compensation of insufficient carbohydrate uptake. Studying these mechanisms might enable us in the future to treat the effects of insufficient carbohydrate uptake at the BBB.

REFERENCES

- Arsov, T., Mullen, S. A., Damiano, J. A., Lawrence, K. M., Huh, L. L., Nolan, M., et al. (2012). Early onset absence epilepsy: 1 in 10 cases is caused by GLUT1 deficiency. *Epilepsia* 53, e204–e207. doi: 10.1111/epi.12007
- Becker, H. M. (2014). "Transport of lactate: characterization of the transporters involved in transport at the plasma membrane by heterologous protein

DATA AVAILABILITY STATEMENT

The raw data supporting the conclusions of this article will be made available by the authors, without undue reservation.

ETHICS STATEMENT

The animal study was reviewed and approved by the Landesuntersuchungsamt Rheinland-Pfalz, Koblenz (23 177-07/A07-2-003 §6).

AUTHOR CONTRIBUTIONS

EM designed and conducted most experiments, helped conceiving the study, and wrote the paper with SS. AW conducted the *Xenopus* experiments together with HB and did some of the fly experiments. HB designed the *Xenopus* experiments and helped conducting them. SS conceived the study, assisted in designing and interpreting experiments, and wrote the paper with EM and obtained funding from the DFG. All authors contributed to the article and approved the submitted version.

FUNDING

The work was supported by grants of the DFG to SS (SFB1009, SCHI 1380/2-1).

ACKNOWLEDGMENTS

We are grateful to C. Klämbt for discussions and critical reading of the manuscript.

SUPPLEMENTARY MATERIAL

The Supplementary Material for this article can be found online at: <https://www.frontiersin.org/articles/10.3389/fnbeh.2020.612430/full#supplementary-material>

expression in *xenopus* oocytes," in *Neuromethods*, eds J. Hirrlinger and H. Waagepetersen (New York, NY: Springer), 25–43.

- Becker, H. M., Bröer, S., and Deitmer, J. W. (2004). Facilitated lactate transport by MCT1 when coexpressed with the sodium bicarbonate cotransporter (NBC) in *xenopus* oocytes. *Biophys. J.* 86, 235–247. doi: 10.1016/S0006-3495(04)74099-0
- Birnbaum, M. J., Haspel, H. C., and Rosen, O. M. (1986). Cloning and characterization of a cDNA encoding the rat brain glucose-transporter

- protein. *Proc. Natl. Acad. Sci. U.S.A.* 83, 5784–5788. doi: 10.1073/pnas.83.16.5784
- Boado, R. J., and Pardridge, W. M. (1993). Glucose deprivation causes posttranscriptional enhancement of brain capillary endothelial glucose transporter gene expression via GLUT1 mRNA stabilization. *J. Neurochem.* 60, 2290–2296. doi: 10.1111/j.1471-4159.1993.tb03516.x
- Broughton, S., Alic, N., Slack, C., Bass, T., Ikeya, T., Vinti, G., et al. (2008). Reduction of DILP2 in *Drosophila* triages a metabolic phenotype from lifespan revealing redundancy and compensation among DILPs. *PLoS ONE* 3:e3721. doi: 10.1371/journal.pone.0003721
- Croset, V., Treiber, C. D., and Waddell, S. (2018). Cellular diversity in the *Drosophila* midbrain revealed by single-cell transcriptomics. *Elife* 7:e34550. doi: 10.7554/eLife.34550
- Daude, N., and Westaway, D. (2012). Shadoo/PrP (Sprn0/0/Prnp0/0) double knockout mice: more than zeroes. *Prion* 6, 420–424. doi: 10.4161/pri.21867
- Davie, K., Janssens, J., Koldere, D., De Waegeneer, M., Pech, U., Kreft, L., et al. (2018). A single-cell transcriptome atlas of the aging *Drosophila* brain. *Cell* 174, 982–998.e20. doi: 10.1016/j.cell.2018.05.057
- De Souza, A. T., Dai, X., Spencer, A. G., Reppen, T., Menzie, A., Roesch, P. L., et al. (2006). Transcriptional and phenotypic comparisons of Ppara knockout and siRNA knockdown mice. *Nucleic Acids Res.* 34, 4486–4494. doi: 10.1093/nar/gkl609
- Desalvo, M. K., Hindle, S. J., Rusan, Z. M., Orng, S., Eddison, M., Halliwill, K., et al. (2014). The *Drosophila* surface glia transcriptome: evolutionary conserved blood-brain barrier processes. *Front. Neurosci.* 8:346. doi: 10.3389/fnins.2014.00346
- Dick, A. P., Harik, S. I., Klip, A., and Walker, D. M. (1984). Identification and characterization of the glucose transporter of the blood-brain barrier by cytochalasin B binding and immunological reactivity. *Proc. Natl. Acad. Sci. U.S.A.* 81, 7233–7237.
- Elfeber, K., Köhler, A., Lutzenburg, M., Osswald, C., Galla, H. J., Witte, O. W., et al. (2004). Localization of the Na⁺-D-glucose cotransporter SGLT1 in the blood-brain barrier. *Histochem. Cell Biol.* 121, 201–207. doi: 10.1007/s00418-004-0633-9
- Enerson, B. E., and Drewes, L. R. (2006). The rat blood-brain barrier transcriptome. *J. Cereb. Blood Flow Metab.* 26, 959–973. doi: 10.1038/sj.jcbfm.9600249
- Engler, C., Kandzia, R., and Marillonnet, S. (2008). A one pot, one step, precision cloning method with high throughput capability. *PLoS ONE* 3:e3647. doi: 10.1371/journal.pone.0003647
- Farrell, C. L., and Pardridge, W. M. (1991). Blood-brain barrier glucose transporter is asymmetrically distributed on brain capillary endothelial luminal and abluminal membranes: an electron microscopic immunogold study. *Proc. Natl. Acad. Sci. U.S.A.* 88, 5779–5783.
- Fehr, M., Lalonde, S., Lager, I., Wolff, M. W., and Frommer, W. B. (2003). *In vivo* imaging of the dynamics of glucose uptake in the cytosol of COS-7 cells by fluorescent nanosensors. *J. Biol. Chem.* 278, 19127–19133. doi: 10.1074/jbc.M301333200
- Gargano, J. W., Martin, I., Bhandari, P., and Grotewiel, M. S. (2005). Rapid iterative negative geotaxis (RING): a new method for assessing age-related locomotor decline in *Drosophila*. *Exp. Gerontol.* 40, 386–395. doi: 10.1016/j.exger.2005.02.005
- Gerhart, D. Z., Levasseur, R. J., Broderius, M. A., and Drewes, L. R. (1989). Glucose transporter localization in brain using light and electron immunocytochemistry. *J. Neurosci. Res.* 22, 464–472. doi: 10.1002/jnr.490220413
- Harik, S. I., Kalara, R. N., Andersson, L., Lundahl, P., and Perry, G. (1990). Immunocytochemical localization of the erythroid glucose transporter: abundance in tissues with barrier functions. *J. Neurosci.* 10, 3862–3872.
- Harris, J. J., Jolivet, R., and Attwell, D. (2012). Synaptic energy use and supply. *Neuron* 75, 762–777. doi: 10.1016/j.neuron.2012.08.019
- Hertenstein, H., McMullen, E., Weiler, A., Volkenhoff, A., Becker, H. M., and Schirmeier, S. (2020). Starvation-induced regulation of carbohydrate transport at the blood-brain barrier is TGF- β -signaling dependent. *bioRxiv*. doi: 10.1101/2020.09.21.306308
- Hindle, S. J., and Bainton, R. J. (2014). Barrier mechanisms in the *Drosophila* blood-brain barrier. *Front. Neurosci.* 8:414. doi: 10.3389/fnins.2014.00414
- Hoffmann, U., Sukhotinsky, I., Eikermann-Haerter, K., and Ayata, C. (2013). Glucose modulation of spreading depression susceptibility. *J. Cereb. Blood Flow Metab.* 33, 191–195. doi: 10.1038/jcbfm.2012.132
- Hummel, T., Attix, S., Gunning, D., and Zipursky, S. L. (2002). Temporal control of glial cell migration in the *Drosophila* eye requires *gilgamesh*, *hedgheg*, and *eye* specification genes. *Neuron* 33, 193–203. doi: 10.1016/S0896-6273(01)00581-5
- Kanamori, Y., Saito, A., Hagiwara-Komoda, Y., Tanaka, D., Mitsumasa, K., Kikuta, S., et al. (2010). The trehalose transporter 1 gene sequence is conserved in insects and encodes proteins with different kinetic properties involved in trehalose import into peripheral tissues. *Insect Biochem. Mol. Biol.* 40, 30–37. doi: 10.1016/j.ibmb.2009.12.006
- Kapogiannis, D., and Mattson, M. P. (2011). Disrupted energy metabolism and neuronal circuit dysfunction in cognitive impairment and Alzheimer's disease. *Lancet. Neurol.* 10, 187–198. doi: 10.1016/S1474-4422(10)70277-5
- Koehn, L. (2020). ABC efflux transporters at blood-central nervous system barriers and their implications for treating spinal cord disorders. *Neural Regen. Res.* 15, 1235–1242. doi: 10.4103/1673-5374.272568
- Koepsell, H. (2020). Glucose transporters in brain in health and disease. *Pflügers Arch. Eur. J. Physiol.* 472, 1299–1343. doi: 10.1007/s00424-020-02441-x
- Kok, F. O., Shin, M., Ni, C. W., Gupta, A., Grosse, A. S., VanImpel, A., et al. (2015). Reverse genetic screening reveals poor correlation between morpholino-induced and mutant phenotypes in zebrafish. *Dev. Cell.* 32, 97–108. doi: 10.1016/j.devcel.2014.11.018
- Kumagai, A. K., Kang, Y.-S., Boado, R. J., and Pardridge, W. M. (1995). Upregulation of blood-brain barrier GLUT1 glucose transporter protein and mRNA in experimental chronic hypoglycemia. *Diabetes* 44, 1399–1404. doi: 10.2337/diab.44.12.1399
- Kuzawa, C. W., Chugani, H. T., Grossman, L. I., Lipovich, L., Muzik, O., Hof, P. R., et al. (2014). Metabolic costs and evolutionary implications of human brain development. *Proc. Natl. Acad. Sci. U.S.A.* 111, 13010–13015. doi: 10.1073/pnas.1323099111
- Laridon, B., Callaerts, P., and Norga, K. (2008). Embryonic expression patterns of *Drosophila* ACS family genes related to the human sialin gene. *Gene Expr. Patterns* 8, 275–283. doi: 10.1016/j.gexp.2007.12.003
- Laughlin, S. B., de Ruyter Van Steveninck, R. R., and Anderson, J. C. (1998). The metabolic cost of neural information. *Nat. Neurosci.* 1, 36–41. doi: 10.1038/236
- Lee, G., and Park, J. H. (2004). Hemolymph sugar homeostasis and starvation-induced hyperactivity affected by genetic manipulations of the adipokinetic hormone-encoding gene in *Drosophila melanogaster*. *Genetics* 167, 311–323. doi: 10.1534/genetics.167.1.311
- Limmer, S., Weiler, A., Volkenhoff, A., Babatz, F., and Klämbt, C. (2014). The *Drosophila* blood-brain barrier: development and function of a glial endothelium. *Front. Neurosci.* 8:365. doi: 10.3389/fnins.2014.00365
- Löscher, W., and Potschka, H. (2005). Blood-brain barrier active efflux transporters: ATP-binding cassette gene family. *NeuroRx* 2, 86–98. doi: 10.1602/neurorx.2.1.86
- Maher, F., Davies-Hill, T. M., Lysko, P. G., Henneberry, R. C., and Simpson, I. A. (1991). Expression of two glucose transporters, GLUT1 and GLUT3, in cultured cerebellar neurons: evidence for neuron-specific expression of GLUT3. *Mol. Cell. Neurosci.* 2, 351–360. doi: 10.1016/1044-7431(91)90066-W
- Maher, F., Vannucci, S. J., and Simpson, I. A. (1994). Glucose transporter proteins in brain. *FASEB J.* 8, 1003–1011. doi: 10.1096/fasebj.8.13.7926364
- Mink, J. W., Blumenshine, R. J., and Adams, D. B. (1981). Ratio of central nervous system to body metabolism in vertebrates: its constancy and functional basis. *Am. J. Physiol. Regul. Integr. Comp. Physiol.* 241, R203–R212. doi: 10.1152/ajpregu.1981.241.3.r203
- Mishra, D., Miyamoto, T., Rezenom, Y. H., Broussard, A., Yavuz, A., Slone, J., et al. (2013). The molecular basis of sugar sensing in *Drosophila* larvae. *Curr. Biol.* 23, 1466–1471. doi: 10.1016/j.cub.2013.06.028
- Nishizaki, T., Kammesheidt, A., Sumikawa, K., Asada, T., and Okada, Y. (1995). A sodium- and energy-dependent glucose transporter with similarities to SGLT1-2 is expressed in bovine cortical vessels. *Neurosci. Res.* 22, 13–22. doi: 10.1016/0168-0102(95)00876-U
- Nishizaki, T., and Matsuoka, T. (1998). Low glucose enhances Na⁺/glucose transport in bovine brain artery endothelial cells. *Stroke* 29, 844–849. doi: 10.1161/01.STR.29.4.844

- Pasco, M. Y., and Léopold, P. (2012). High sugar-induced insulin resistance in *Drosophila* relies on the lipocalin Neural Lazarillo. *PLoS ONE* 7:e36583. doi: 10.1371/journal.pone.0036583
- Patching, S. G. (2016). Glucose transporters at the blood-brain barrier: function, regulation and gateways for drug delivery. *Mol. Neurobiol.* 54, 1046–1077. doi: 10.1007/s12035-015-9672-6
- Rehni, A. K., and Dave, K. R. (2018). Impact of hypoglycemia on brain metabolism during diabetes. *Mol. Neurobiol.* 55, 9075–99088. doi: 10.1007/s12035-018-1044-6
- Rodrigues, F., Thuma, L., and Klämbt, C. (2012). The regulation of glial-specific splicing of Neurexin IV requires HOW and Cdk12 activity. *Development* 139, 1765–1776. doi: 10.1242/dev.074070
- Rossi, A., Kontarakis, Z., Gerri, C., Nolte, H., Hölper, S., Krüger, M., et al. (2015). Genetic compensation induced by deleterious mutations but not gene knockdowns. *Nature* 524, 230–233. doi: 10.1038/nature14580
- Schmidt, I., Thomas, S., Kain, P., Risse, B., Naffin, E., and Klämbt, C. (2012). Kinesin heavy chain function in *Drosophila* glial cells controls neuronal activity. *J. Neurosci.* 32, 7466–7476. doi: 10.1523/JNEUROSCI.0349-12.2012
- Simpson, I. A., Appel, N. M., Hokari, M., Oki, J., Holman, G. D., Maher, F., et al. (1999). Blood-brain barrier glucose transporter: effects of hypo- and hyperglycemia revisited. *J. Neurochem.* 72, 238–247. doi: 10.1046/j.1471-4159.1999.0720238.x
- Simpson, I. A., Vannucci, S. J., DeJoseph, M. R., and Hawkins, R. A. (2001). Glucose transporter asymmetries in the bovine blood-brain barrier. *J. Biol. Chem.* 276, 12725–12729. doi: 10.1074/jbc.M010897200
- Sivitz, W., DeSautel, S., Walker, P. S., and Pessin, J. E. (1989). Regulation of the glucose transporter in developing rat brain. *Endocrinology* 124, 1875–1880. doi: 10.1210/endo-124-4-1875
- Stephan, R., Grevelhörster, A., Wenderdel, S., Klämbt, C., and Bogdan, S. (2008). Abi induces ectopic sensory organ formation by stimulating EGFR signaling. *Mech. Dev.* 125, 183–195. doi: 10.1016/j.mod.2007.12.002
- Stork, T., Engelen, D., Krudewig, A., Silies, M., Bainton, R. J., and Klämbt, C. (2008). Organization and function of the blood brain barrier in *Drosophila*. *J. Neurosci.* 28, 587–597. doi: 10.1523/JNEUROSCI.4367-07.2008
- Sulem, P., Helgason, H., Oddson, A., Stefansson, H., Gudjonsson, S. A., Zink, F., et al. (2015). Identification of a large set of rare complete human knockouts. *Nat. Genet.* 47, 448–452. doi: 10.1038/ng.3243
- Takanaga, H., Chaudhuri, B., and Frommer, W. B. (2008). GLUT1 and GLUT9 as major contributors to glucose influx in HepG2 cells identified by a high sensitivity intramolecular FRET glucose sensor. *Biochim. Biophys. Acta Biomembr.* 1778, 1091–1099. doi: 10.1016/j.bbame.2007.11.015
- Vemula, S., Roder, K. E., Yang, T., Bhat, G. J., Thekkumkara, T. J., and Abbruscato, T. J. (2009). A functional role for sodium-dependent glucose transport across the blood-brain barrier during oxygen glucose deprivation. *J. Pharmacol. Exp. Ther.* 328, 487–495. doi: 10.1124/jpet.108.146589
- Volkenhoff, A., Hirrlinger, J., Kappel, J. M., Klämbt, C., and Schirmeier, S. (2018). Live imaging using a FRET glucose sensor reveals glucose delivery to all cell types in the *Drosophila* brain. *J. Insect Physiol.* 106, 55–64. doi: 10.1016/j.jinsphys.2017.07.010
- Volkenhoff, A., Weiler, A., Letzel, M., Stehling, M., Klämbt, C., and Schirmeier, S. (2015). Glial glycolysis is essential for neuronal survival in *Drosophila*. *Cell Metab.* 22, 437–447. doi: 10.1016/j.cmet.2015.07.006
- Weiler, A., Volkenhoff, A., Hertenstein, H., and Schirmeier, S. (2017). Metabolite transport across the mammalian and insect brain diffusion barriers. *Neurobiol. Dis.* 107, 15–31. doi: 10.1016/j.nbd.2017.02.008
- Weizmann, R., Hammonds, A. S., and Celniker, S. E. (2009). Determination of gene expression patterns using high-throughput RNA *in situ* hybridization to whole-mount *Drosophila* embryos. *Nat. Protoc.* 4, 605–618. doi: 10.1038/nprot.2009.55
- Wyatt, G. R., and Kalf, G. F. (1957). The chemistry of insect hemolymph: II. Trehalose and other carbohydrates. *J. Gen. Physiol.* 40, 833–847.
- Yildirim, K., Petri, J., Kottmeier, R., and Klämbt, C. (2019). *Drosophila* glia: few cell types and many conserved functions. *Glia* 67, 5–26. doi: 10.1002/glia.23459
- Yu, A. S., Hirayama, B. A., Timbol, G., Liu, J., Diez-Sampedro, A., Kepe, V., et al. (2013). Regional distribution of SGLT activity in rat brain *in vivo*. *Am. J. Physiol. Cell Physiol.* 304, C240–C247. doi: 10.1152/ajpcell.00317.2012

Conflict of Interest: The authors declare that the research was conducted in the absence of any commercial or financial relationships that could be construed as a potential conflict of interest.

Copyright © 2021 McMullen, Weiler, Becker and Schirmeier. This is an open-access article distributed under the terms of the Creative Commons Attribution License (CC BY). The use, distribution or reproduction in other forums is permitted, provided the original author(s) and the copyright owner(s) are credited and that the original publication in this journal is cited, in accordance with accepted academic practice. No use, distribution or reproduction is permitted which does not comply with these terms.